

Numerical simulation for laser-induced breakdown thresholds and plasma formation in water

Hongchao Zhang (张宏超), Jian Lu (陆建), Xiaowu Ni (倪晓武), and Zhonghua Shen (沈中华)

Department of Applied Physics, Nanjing University of Science and Technology, Nanjing 210094

Two models to calculate the irradiance threshold for laser-induced breakdown for water have been introduced. Both of the models have been incorporated into a computer code and code results compared to experimentally measured irradiance threshold for breakdown of pure water by nanosecond, picosecond and femtosecond laser pulses in the visible and near-infrared. The result shows that the second one has a wider range than first one to agree with the experiment data. For nanosecond laser pulses, the generation of free electrons in distilled water is initiated by multiphoton ionization but then dominated by cascade ionization. For shorter laser pulses, multiphoton ionization gains ever more importance, and collision and recombination losses during breakdown diminish. The threshold near infrared is more depend on the initial electrons.

OCIS codes: 140.0140, 140.3440, 260.5210, 350.5400.

The interaction of high-power laser radiation with transparent media can lead to a plasma formation. When the free electron density exceeds a critical value of $10^{18} - 10^{20} \text{ cm}^{-3}$ ^[1], it is called optical breakdown or laser induced breakdown (LIB). Two mechanisms, direct ionization of the medium by multiphoton absorption or avalanche ionization via inverse bremsstrahlung absorption, can lead to LIB. Avalanche ionization requires an initial quasi-free seed electron in the focal volume and long pulse duration, whereas multiphoton ionization does not need seed electrons and can occur during ultra short laser pulse duration. In pure media, the breakdown of the medium needs the Multiphoton ionization providing the "seed electron"^[1].

The time evolution of the electron density under the influence of the laser pulse, in a simplified way, is described by

$$\frac{d\rho}{dt} = \left(\frac{d\rho}{dt}\right)_m + \eta_{\text{casc}}\rho - g\rho - \eta_{\text{rec}}\rho^2. \quad (1)$$

The first two terms on the right-hand side describe the production of free electrons through multiphoton and cascade ionization. The remaining terms account for the diffusion of electrons out of the focal volume and recombination. For a detailed description of the individual terms of Eq. (1) the reader is referred to Refs. [1]–[3].

Based on this simple rate equation, an analytic, first-order model was been developed by Kennedy to calculate irradiance thresholds for LIB in condensed media. To calculated the threshold Kennedy gave some somewhat arbitrarily hypothesis^[1]. The breakdown thresholds also

can be numerically solved by calculating the evolution of the electron density for laser pulses with a Gaussian time variation, which was called the rate equation model^[3].

Table 1 lists some values of breakdown thresholds determined experimentally for distilled and filtered water^[4–6], along with thresholds calculated for pure water using the two models. The threshold predicted by the rate equation model agrees very well with the measured for various duration pulses. The first-order model did not agree so well, especially for 76 ns duration. It is because it is assumed a time $t = \tau_L/10$ for the generation of the initial electrons by multiphoton ionization, and has not consider the electron losses during his phase. With increasing the pulse duration, the losses electrons can never be ignored, especially for nanosecond and visible wavelengths. The rate equation models do not have this problem, which assumed that a statistical average of 0.5 electrons exists within the focal volume that cascades ionization start.

Figure 1 shows the evolution of the free electron density $\rho(t)$ in pure water for pulse durations at wavelength of 580 and 1064 ns. The curves reveal the relative importance of multiphoton and cascade ionization and their interplay in the course of breakdown. Multiphoton ionization becomes increasingly important with decreasing wavelengths and pulse durations. It is because a few photons are required to ionization a free electron through multiphoton ionization at short wavelengths, and a higher ionization rate is required to reach the critical electron density during the shorter pulse duration.

Table 1. Comparison of Measured Breakdown Thresholds (I_{th}) and Thresholds Predicted by the First-order (I_{rate1}) and the Rate Equation Model (I_{rate2})

τ_L (ps)	λ (nm)	d (μm)	I_{th} (10^{11} W/cm^2)	I_{rate1} (10^{11} W/cm^2)	I_{rate2} (10^{11} W/cm^2)	Ref. of I_{th}
76×10^3	750	20	0.2	0.026	0.19	Ref. [4]
6×10^3	1064	7.7	0.5	0.76	0.53	Ref. [6]
6×10^3	532	5.3	0.3	0.06	0.41	Ref. [6]
30	1064	4.7	4.5	3.76	4.4	Ref. [6]
30	532	3.4	3.8	1.4	3.6	Ref. [6]
3	580	5.0	8.5	12.4	9.1	Ref. [4]
0.3	580	5.0	47.6	73.9	52.6	Ref. [5]
0.1	580	4.4	111	205.1	111.5	Ref. [4]

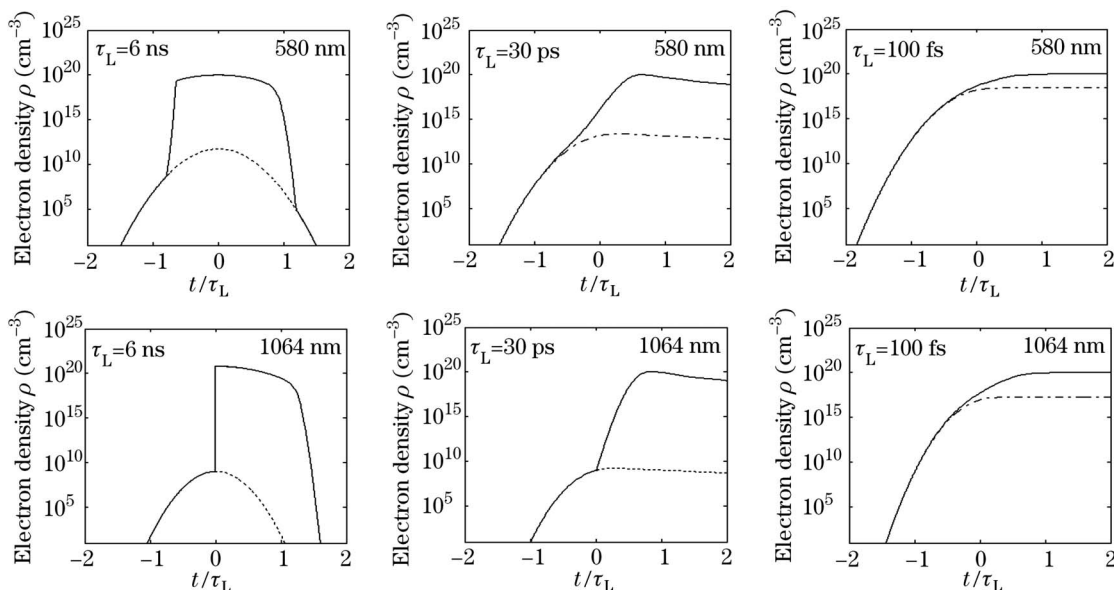


Fig. 1. Evolution of the free electron density at breakdown threshold for different pulse durations and different wavelengths. The calculations were performed for breakdown in pure water, and a spot size of $5 \mu\text{m}$. Besides the total free electron concentration (solid curve), the concentration due to multiphoton absorption (dotted curve) is plotted as a function of time. The time axis has been normalized to the laser pulse duration τ_L .

The large majority of free electrons are always created by cascade ionization. It is because the cascade ionization rate is proportional to the density of free electrons already that produced in the course of the laser pulse, whereas the multiphoton ionization rate is independent of $\rho(t)$. The initial part of the breakdown process is dominated by multiphoton processes, however as soon as the first electron is generated in the focal volume, the cascade ionization can start, and immediately dominate the production of free electrons. For nanosecond, when the electron density is close to the critical electron density, a dynamic equilibrium between the free electron generation and electrons is established. During this phase, the electron density grows very smoothly and follows the time evolution of the irradiance during the laser pulse. On the trailing edge of the laser pulse, the electrons recombination can no longer be compensated for by the production of free electrons because of the decreasing irradiance, thus the free electron density decreases rapidly at the end of the laser ionization. However the influence of recombination becomes negligible for pulse durations of 30 fs and shorter because the recombination is then slow compared to the laser pulse duration. For nanosecond pulse laser in near-infrared, the curve is very sharp at peak of the laser irradiance. It is because more photons are required for multiphoton ionization to provide the initial seed electrons.

Both of the models had somewhat arbitrarily assumed a constant number of initial electrons $N_{0\text{min}}$ to start the cascade. To make a better understand of the assumptions of the number start electrons how influence of the calculated threshold values, we had calculated the threshold at various number of start electrons based on the rate equation model.

Figure 2 shows the irradiance threshold as a function of pulse duration for pure water with different $N_{0\text{min}}$. For infrared wavelengths, the calculated threshold depends

$N_{0\text{min}}$ strongly, especially for nanosecond pulse duration. Whereas for visible wavelengths, $N_{0\text{min}}$ has nothing to do with the calculated thresholds even at $N_{0\text{min}} = 100$. Fig. 3 shows the detail of the dependence between calculated threshold and $N_{0\text{min}}$ at nanosecond pulse duration. With increasing the $N_{0\text{min}}$ the curve for 1064 nm becomes smooth. It is because $N_{0\text{min}}$ becomes more easily offered by multiphoton ionization with increasing the threshold. The number of start electrons influences the calculated threshold values for infrared wavelengths and pulse duration about above 20 ps.

Figure 4 shows evolution of the free electron density at breakdown threshold for different number of initial electrons at nanosecond pulse duration. For visible wavelength, the dynamic equilibrium between the free electron generation and electron losses establishes before the peak of the laser pulse, $N_{0\text{min}}$ only influences the balance establishing time and the threshold is determined by the irradiance to overcome the recombination losses at

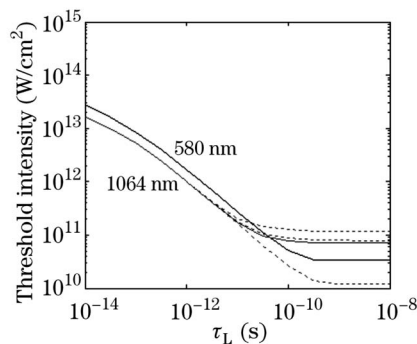


Fig. 2. Threshold irradiance for LIB as a function of pulse duration for 580 nm (top solid curve), for 1064 nm in pure water (bottom solid curve), and for 1064 nm with $N_{0\text{min}} = 0$, $N_{0\text{min}} = 1$, $N_{0\text{min}} = 10$ (dotted curve, bottom to top) in pure water, where $N_{0\text{min}}$ is the assumed number of “seed electrons”. $\rho_{\text{cr}} = 10^{20} \text{ cm}^{-3}$, spot size $5 \mu\text{m}$.

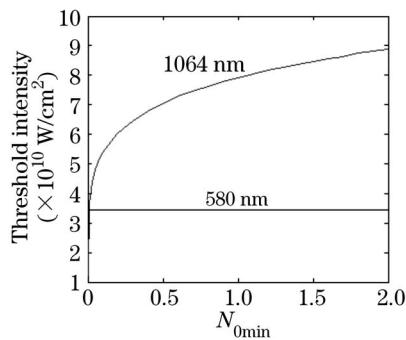


Fig. 3. Threshold irradiance for LIB as a function of assumed number of "seed electrons" for 580 and 1064 nm, $\rho_{cr} = 10^{20} \text{ cm}^{-3}$, spot size $5 \mu\text{m}$, $\tau_L = 6 \text{ ns}$.

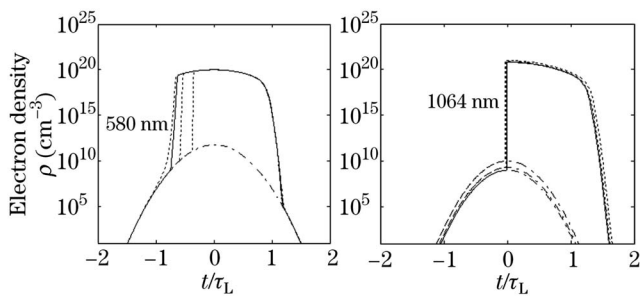


Fig. 4. Evolution of the free electron density at breakdown threshold for different number of initial electrons. Besides the total free electron concentration, the concentration due to multiphoton absorption (dash dot curve) is plotted as a function of time. The time axis has been normalized to the laser pulse duration τ_L . $\rho_{cr} = 10^{20} \text{ cm}^{-3}$, spot size $5 \mu\text{m}$, $\tau_L = 6 \text{ ns}$.

ρ_{cr} . For infrared wavelengths, only at the peak of the pulse the initial electrons can be generated by the multiphoton ionization. The threshold thus is determined by the irradiance of the multiphoton ionization which should provide the seed electrons at the peak of the pulse. For nanosecond and femtosecond laser pulse duration,

the figures also have been calculated which not show here. With decreasing the pulse duration, threshold irradiance must increase to induced breakdown during a shorter time. Multiphoton ionization therefore becomes important. The seed electrons become more easily being offered by the multiphoton, when the threshold that depends on the initial electrons becomes very weak. However for infrared wavelengths about above 20 ps, the threshold is still influence by N_{0min} . For shorter, the dependence disappeared.

In conclusion, the rate equation model has a wider range than the first-order to agree with the experiment data. For visible wavelengths, the calculated threshold is determined by the irradiance to overcome the recombination losses at ρ_{cr} . For infrared wavelengths, it is determined by the irradiance of the multiphoton ionization which should provide the seed electrons at the peak of the pulse. The influence of the assumptions of the number on the threshold is notable only for infrared wavelengths and pulse durations about above 20 ps.

X. Ni is the author to whom the correspondence should be addressed, his e-mail address is nxw@mail.njust.edu.cn.

References

1. P. K. Kennedy, S. A. Boppart, D. X. Hammer, B. A. Rockwell, G. D. Noojin, and W. P. Roach, *IEEE J. Quantum Electron.* **31**, 2250 (1995).
2. F. Williams, S. P. Varma, and S. Hillenius, *J. Chem. Phys.* **64**, 1549 (1976).
3. J. Noack, A. Voge, *IEEE J. Quantum Electron.* **35**, 1155 (1999).
4. J. Noack, A. Vogel, D. X. Hammer, G. D. Noojin, and B. A. Rockwell, *J. Appl. Phys.* **84**, 7488 (1998).
5. A. Vogel, J. Noack, K. Nahen, D. Theisen, S. Busch, U. Parlitz, D. X. Hammer, G. D. Noojin, B. A. Rockwell, and R. Birngruber, *Appl. Phys. B* **68**, 271 (1999).
6. A. Vogel, K. Nahen, D. Theisen, and J. Noack, *IEEE J. Sel. Top. Quantum Electron.* **2**, 847 (1996).